

Exceptionally efficient organic light emitting devices using high refractive index substrates

Saso Mladenovski,^{1,*} Kristiaan Neyts,¹
Domagoj Pavicic,² Ansgar Werner² and Carsten Rothe²

¹Electronics and Information Systems Department, Ghent University, Sint-Pietersnieuwstraat 41, B-9000 Gent, Belgium

²NOVALED AG, Tatzberg 49, 01307 Dresden, Germany

*Saso.Mladenovski@elis.ugent.be

Abstract: Organic light emitting devices (OLEDs) are now used in commercial cell phones and flat screen displays, but may become even more successful in lighting applications, in which large area, high efficiency, long lifetime and low cost are essential. Due to the relatively high refractive index of the organic layers, conventional planar bottom emitting OLEDs have a low outcoupling efficiency. Various approaches for enhancing the optical outcoupling efficiency of bottom emitting OLEDs have been introduced in the literature. In this paper we demonstrate a green bottom emitting OLED with a record external quantum efficiency (42%) and luminous efficacy (183 lm/W). This OLED is based on a high index substrate and a thick electron transport layer (ETL) which uses electrical doping. The efficient light outcoupling is modeled by optical simulations.

©2009 Optical Society of America

OCIS codes: (230.3670) Light-emitting diodes; (310.6845) Thin film devices and applications; (310.6860) Thin films, optical properties; (160.4890) Organic materials

References and links

1. C. W. Tang, and S. A. VanSlyke, "Organic electroluminescent diodes," *Appl. Phys. Lett.* **51**(12), 913–915 (1987).
2. H. Peng, Y. L. Ho, X.-J. Yu, M. Wong, and H.-S. Kwok, "Coupling Efficiency Enhancement in Organic Light-Emitting Devices Using Microlens Array - Theory and Experiment," *IEEE J. Disp. Technol.* **1**(2), 278–282 (2005).
3. S. Möller, and S. R. Forrest, "Improved light out-coupling in organic light emitting diodes employing ordered microlens arrays," *J. Appl. Phys.* **91**(5), 3324–3327 (2002).
4. J. Lim, S. S. Oh, D. Y. Kim, S. H. Cho, I. T. Kim, S. H. Han, H. Takezoe, E. H. Choi, G. S. Cho, Y. H. Seo, S. O. Kang, and B. Park, "Enhanced out-coupling factor of microcavity organic light-emitting devices with irregular microlens array," *Opt. Express* **14**(14), 6564–6571 (2006).
5. C. F. Madigan, M.-H. Lu, and J. C. Sturm, "Improvement of output coupling efficiency of organic light-emitting diodes by backside substrate modification," *Appl. Phys. Lett.* **76**(13), 1650–1652 (2000).
6. T. Tsutsui, M. Yahiro, H. Yokogawa, K. Kawano, and M. Yokoyama, "Doubling Coupling-Out Efficiency in Organic Light-Emitting Devices Using a Thin Silica Aerogel Layer," *Adv. Mater.* **13**(15), 1149–1152 (2001).
7. S. K. So, W. K. Choi, L. M. Leung, and K. Neyts, "Interference effects in bilayer organic light-emitting diodes," *Appl. Phys. Lett.* **74**(14), 1939–1941 (1999).
8. Y.-C. Kim, S.-H. Cho, Y.-W. Song, Y.-J. Lee, Y.-H. Lee, and Y. R. Do, "Planarized SiNx/spin-on-glass photonic crystal organic light-emitting diodes," *Appl. Phys. Lett.* **89**(17), 173502 (2006).
9. Y.-J. Lee, S.-H. Kim, J. Huh, G.-H. Kim, Y.-H. Lee, S.-H. Cho, Y.-C. Kim, and Y. R. Do, "A high-extraction-efficiency nanopatterned organic light-emitting diode," *Appl. Phys. Lett.* **82**(21), 3779–3781 (2003).
10. Y. Sun, and S. R. Forrest, "Enhanced light out-coupling of organic light-emitting devices using embedded low-index grids," *Nat. Photonics* **2**(8), 483–487 (2008).
11. T. Nakamura, N. Tsutsumi, N. Juni, and H. Fujii, "Thin-film waveguiding mode light extraction in organic electroluminescent device using high refractive index substrate," *J. Appl. Phys.* **97**(5), 054505 (2005).
12. H. J. Peng, Y. L. Ho, C. F. Qui, M. Wong and H. S. Kwok, "Coupling Efficiency Enhancement of Organic Light Emitting Devices with Refractive Microlens Array on High Index Glass Substrate," *SID' 04 Digest*, **35**, 158–161 (2004).
13. D. Tanaka, H. Sasabe, Y.-J. Li, S.-J. Su, T. Takeda, and J. Kido, "Ultra High Efficiency Green Organic Light-Emitting Devices," *Jpn. J. Appl. Phys.* **46**(1), L10–L12 (2007).
14. K. Neyts, "Simulation of light emission from thin-film microcavities," *J. Opt. Soc. Am. A* **15**(4), 962–971 (1998).

15. K. Neyts, "Microcavity effects and the outcoupling of light in displays and lighting applications based on thin emitting films," *Appl. Surf. Sci.* **244**(1-4), 517–523 (2005).
16. H. Riel, S. Karg, T. Beirlein, W. Rieß, and K. Neyts, "Tuning the emission characteristics of top-emitting organic light-emitting devices by means of a dielectric capping layer: An experimental and theoretical study," *J. Appl. Phys.* **94**(8), 5290–5296 (2003).
17. J. Blochwitz, M. Pfeiffer, T. Fritz, and K. Leo, "Low voltage organic light emitting diodes featuring doped phthalocyanine as hole transport material," *Appl. Phys. Lett.* **73**(6), 729–731 (1998).
18. M. A. Baldo, S. Lamansky, P. E. Burrows, M. E. Thompson, and S. R. Forrest, "Very high efficiency green organic light-emitting devices based on electrophosphorescence," *Appl. Phys. Lett.* **75**(1), 4–6 (1999).
19. G. He, O. Schneider, D. Qin, X. Zhou, M. Pfeiffer, and K. Leo, "Very high-efficiency and low voltage phosphorescent organic light-emitting diodes based on a p-i-n junction," *J. Appl. Phys.* **95**(10), 5773–5777 (2004).
20. C.-L. Lin, T.-Y. Cho, C.-H. Chang, and C.-C. Wu, "Enhancing light outcoupling of organic light-emitting devices by locating emitters around the second antinode of the reflective metal electrode," *Appl. Phys. Lett.* **88**(8), 081114 (2006).
21. P. Wellmann, M. Hofmann, O. Zeika, A. Werner, J. Birnstock, R. Meerheim, G. He, K. Walzer, M. Pfeiffer, and K. Leo, "High-efficiency p-i-n organic light-emitting diodes with long lifetime," *J. Soc. Inf. Disp.* **13**(5), 393–397 (2005).
22. J. Birnstock, M. Hofmann, S. Murano, M. Vehse, J. Blochwitz-Nimoth, Q. Huang, G. He, M. Pfeiffer and K. Leo, "Novel OLEDs for Full Color Display with Highest Power Efficiencies and Long Lifetime," *SID' 05 Dig.* **36**, 40–43 (2005).
23. J. Birnstock, A. Lux, M. Ammann, P. Wellmann, M. Hofmann and T. Stübinger, "Novel Materials and Structures for Highly-Efficient, Temperature-Stable, and Long-Living AM OLED Displays," *SID' 06 Dig.* **37**, 1866–1869 (2006).
24. K. Neyts, M. Marescaux, A. U. Nieto, A. Elschner, W. Lövenich, K. Fehse, Q. Huang, K. Walzer, and K. Leo, "Inhomogeneous luminance in organic light emitting diodes related to electrode resistivity," *J. Appl. Phys.* **100**(11), 114513 (2006).
25. S. Reineke, G. Schwartz, K. Walzer, and K. Leo, "Reduced efficiency roll-off in phosphorescent organic light emitting diodes by suppression of triplet-triplet annihilation," *Appl. Phys. Lett.* **91**(12), 123508 (2007).
26. Q. Huang, S. Reineke, K. Walzer, M. Pfeiffer, and K. Leo, "Quantum efficiency enhancement in top-emitting organic light-emitting diodes as a result of enhanced intrinsic quantum yield," *Appl. Phys. Lett.* **89**(26), 263512 (2006).
27. K.-B. Kim, Y.-H. Tak, Y.-S. Han, K.-H. Baik, M.-H. Yoon, and M.-H. Lee, "Relationship between Surface Roughness of Indium Tin Oxide and Leakage Current of Organic Light-Emitting Diode," *Jpn. J. Appl. Phys.* **42**(Part 2, No. 4B), L438–L440 (2003).

1. Introduction

From the first devices [1] until today, organic light-emitting devices (OLEDs) have known a rapid development, leading to a range of commercial applications. For lighting, one of the most important parameters is the luminous efficacy: the ratio of emitted lumens over dissipated power. In conventional bottom emitting OLEDs, the light is emitted through the substrate, which usually has a lower refractive index ($n_{\text{substrate}} = 1.5$) than the organic layers ($n_{\text{organic}} \approx 1.8$). For a flat OLED, a substantial fraction of the light is trapped inside the organic layers due to total internal reflection (TIR). In addition, there is also TIR at the substrate/air interface. As a result, the outcoupling efficiency $\eta_{\text{out}}^{\text{air}}$ (the fraction of generated light that reaches air) is low.

Various approaches for enhancing the optical outcoupling efficiency of bottom emitting OLEDs have been introduced in the literature. Often, the planar substrate/air interface is modified in order to reduce repeated TIR: by using a microlens array [2–4] or a large half sphere lens [5] on the substrate surface. Other outcoupling methods try to extract the light trapped in the organic/ITO layers. This can be realized by using a low refractive index ($n = 1.03$) porous aerogel [6], microcavity effects [7], photonic crystals [8,9], or an embedded low-index grid [10]. Some of these methods have drawbacks such as a reduction in electrical efficiency, a decrease in lifetime, a viewing angle dependent color, and/or an increase in production cost. In this work we use a high refractive index substrate to couple the light from the organic layers efficiently into the substrate. This approach has been proposed in the past [11,12] but was not yet confirmed experimentally. In this work we demonstrate the potential of high index substrates theoretically and experimentally. A record [13] external quantum efficiency of 42% and luminous efficacy of 183 lm/W was measured for a green bottom emitting OLED at 1000 cd/m².

In Section 2 we explain the optical model used for carrying out simulations. Section 3 describes the device fabrication process and measurement methods. In Section 4 we show the results from the simulation and measurements of OLEDs on both regular glass substrates and high index substrates, and make a comparison of the two. Finally the conclusions are presented in Section 5.

2. Optical model and simulations

The optical performance of the OLEDs has been simulated using an optical model based on a plane wave expansion of the dipole radiation [14,15]. It assumes a one dimensional structure for the OLED, because the lateral dimensions are much larger than the thickness. The emission is modeled by considering an ensemble of incoherent classical electrical dipole antennas with random orientation, and the probability for emitting a photon in a certain direction is considered to be proportional to the power radiated by the antenna ensemble. The light emitted by a dipole antenna is partially or totally reflected at the interfaces between the different layers in the OLED. The model takes into account wide-angle interference and multiple-beam interference which occur in the structure because of the reflections. As the emission arises from small molecules, it is important to average over all possible dipole orientations (randomly oriented dipoles), as was proposed and confirmed in earlier work [7,16]. The simulation model includes the emission into plane and evanescent waves in the emitting layer as described elsewhere [14,15].

The outcoupling efficiency for a given OLED structure is defined as the fraction of the total light generated by the ensemble of dipole antennas that reaches the substrate ($\eta_{out}^{substrate}$) or air (η_{out}^{air}). To determine the amount of light that exits from the substrate into air, we assume either total internal reflection or partial reflection at the substrate/air interface, and neglect contributions from multiple reflections. The angular distribution of the light emitted into the substrate or into air can be determined with the same model. The input parameters of the simulation model are the thicknesses and wavelength-dependent (complex) refractive indices for the different layers.

3. Device fabrication and measurements

Large emitter-electrode distances are achieved by using electrically doped charge transport layers, which feature externally high conductivities (typically 10^{-5} S/cm). This allows us to demonstrate high luminous efficacy and to be able to compare the efficiencies of OLEDs with different emitter-cathode distances but identical electrical properties. Details about the electrical doping technology called "PIN" are given in [17].

The OLED stack was based on a phosphorescent green double-emission structure with Ir(ppy)₃, for which high luminous efficacies have already been demonstrated [13,18]. The structure of the device is the following (Fig. 1): indium tin oxide (ITO)/p-type-doped hole transport layer (HTL)/electron blocking layer (EBL)/hole transporting emission layer (EMLI)/electron transporting emission layer (EMLII)/hole blocking layer (HBL)/n-type-doped electron transport layer (ETL)/silver cathode. For this stack the charge carrier recombination zone is pin pointed at the interface between the two emission layers, which has been shown previously [19]. All devices were prepared by thermal evaporation of different organic layers in ultrahigh vacuum with base pressure 10^{-8} mbar. The PIN structure was applied onto an ITO coated glass substrate ($n_{substrate} = 1.5$) or a high index sapphire substrate ($n_{substrate} = 1.8$), which are patterned for OLEDs with an emitting area of $21 \times 21\text{mm}^2$ or $2.5 \times 2.5\text{mm}^2$ correspondingly. The devices were encapsulated with glass under an inert gas atmosphere.

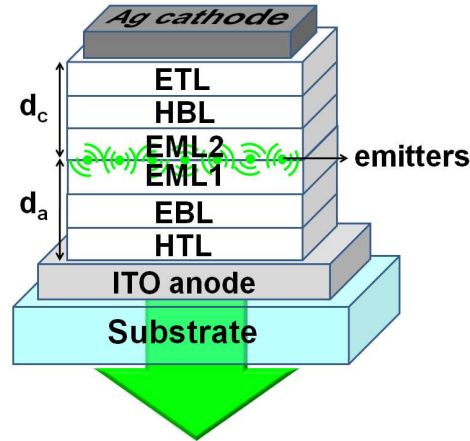


Fig. 1. Structure of the organic light-emitting device (OLED). Layers from top to bottom: silver cathode, electron-transport layer (ETL), hole-blocking layer (HBL), emission layers (EML2 & EML1), electron-blocking layer (EBL), hole-transport layer (HTL). Emitters are located at the EML1/EML2 interface. The distances of emitters from the cathode and the anode are d_c and d_a respectively.

The luminous efficacy and quantum efficiency in air are measured by placing the OLED inside an integrating sphere, and covering the edges of the substrate with an absorbing material. In this way, the light that is leaving the OLED through the edge of the substrate is not included. Similarly, the luminous efficacy and quantum efficiency in the substrate are measured by placing the samples in an integrating sphere with an index matched half sphere lens (much larger than the OLED device) on top of the substrate. The half sphere is attached by using an index matching immersion oil. The angular distribution of the light intensity in the substrate is measured by attaching a half sphere with high refractive index to the substrate and using an advanced Autronic Melchior's goniometer, which integrates over the whole emission spectrum.

4. Results

4.1 OLED on regular glass substrate

First we investigate how the integrated emission of a green bottom emitting OLED (Fig. 1) on a standard glass substrate ($n_{\text{substrate}} = 1.5$) depends on the distances between the recombination zone and the silver cathode (d_c), respectively the ITO anode (d_a) (see Fig. 1). The optical modeling is based on the plane wave expansion of the radiation from a randomly oriented dipole antenna, presented in Section 2. Figures 2(a) and 2(b) show the numerically simulated outcoupling efficiency in air $\eta_{\text{out}}^{\text{air}}$ and in the substrate $\eta_{\text{out}}^{\text{substrate}}$ for monochromatic light with wavelength $\lambda = 530\text{nm}$. This is the central wavelength of the green emission spectrum of $\text{Ir}(\text{ppy})_3$, which is then used in the structure of Fig. 1. Figures 2(a) and 2(b) illustrate that the two efficiencies depend strongly on d_c and weakly on d_a . The dependency of d_c is ascribed to wide-angle interference between the dipole and its mirror image. Figure 2(a) also shows that $\eta_{\text{out}}^{\text{air}}$ is considerably higher for the second maximum with respect to d_c (around $d_c = 220\text{nm}$ and $d_a = 60\text{nm}$), than for the first maximum (around $d_c = 70\text{nm}$ and $d_a = 50\text{nm}$), namely $\eta_{\text{out}}^{\text{air}} = 24\%$ instead of $\eta_{\text{out}}^{\text{air}} = 18\%$. For $\eta_{\text{out}}^{\text{substrate}}$ (Fig. 2(b)), the global maximum occurs at $d_c = 230\text{nm}$ and $d_a = 80\text{nm}$ ($\eta_{\text{out}}^{\text{substrate}} = 42\%$). The reason for the larger $\eta_{\text{out}}^{\text{substrate}}$ at the second maximum is that a larger d_c (i.e. thicker ETL) reduces the coupling between evanescent waves generated by the dipole antenna and the silver cathode. In conclusion, we expect that the external efficiency for an OLED on glass can be improved by about 30% by using thick ETL

layers. The advantage of using a thicker ETL and operating in the second maximum was already reported in literature [20].

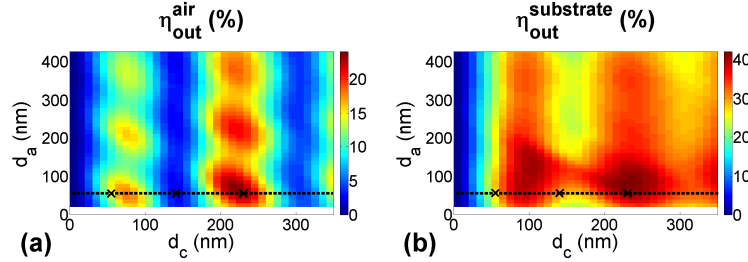


Fig. 2. Simulated outcoupling efficiency in air η_{out}^{air} (a) and in the substrate $\eta_{out}^{substrate}$ (b) for OLEDs with a regular glass substrate as a function of d_c and d_a i.e. the distances between the emitters and the cathode and the anode respectively. The dashed line ($d_a = 60$ nm) indicates the parameters for the fabricated devices. The three crosses represent the parameters for which the angular distribution is shown in Fig. 4.

To study the influence of d_c on the outcoupling efficiencies η_{out}^{air} and $\eta_{out}^{substrate}$ a series of green phosphorescent OLED samples (area 21x21mm²) has been fabricated with d_c between 50nm to 250nm, keeping d_a constant at 60nm. The deposition is based on doping technology [21–23], allowing the use of thick ETLs with high conductivity. This highly conductive ETL ensures a good balance of electrons and holes and leads to constant internal quantum efficiency, independent of d_c . As a result, the variations in the measured external efficiency can be ascribed to variations in the optical outcoupling efficiency. The comparison between the measured luminous efficacies and simulated outcoupling efficiencies η_{out}^{air} and $\eta_{out}^{substrate}$, is shown in Fig. 3. The luminous efficacies in air and in the substrate are measured with an integrating sphere at a luminance of 1000 cd/m². For the measurement of the emission in the substrate, a large index-matched half-sphere lens was attached to the substrate. Figure 3 shows that the simulated outcoupling efficiencies and the measured luminous efficacies have the same dependency on d_c and therefore we can conclude that the internal power efficiency is nearly independent of d_c . For the most efficient OLED ($d_c = 230$ nm and $d_a = 60$ nm) measured at 1000 cd/m², the luminous efficacies are 61 lm/W in air and 102 lm/W in the substrate corresponding to external quantum efficiencies of 16% and 27% respectively.

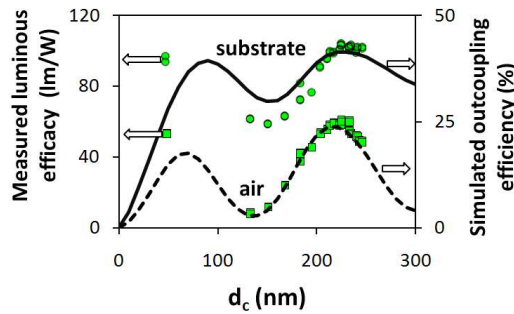


Fig. 3. Measured luminous efficacy (points) in air and in the substrate and simulated outcoupling efficiency (lines) in air η_{out}^{air} and in the substrate $\eta_{out}^{substrate}$ as a function of d_c (with constant $d_a = 60$ nm).

At a luminance level of 1000cd/m² the measured luminous efficacies are lower than for 100cd/m². This is partly due to the voltage drop in the anode [24] (high current density through the resistive ITO) and partly to the efficiency roll-off [25] in this phosphorescent OLED at high current density. When the same OLED is measured at a luminance level of

100cd/m² we find even higher values for the luminous efficacy in air and in the substrate: 75 lm/W and 122 lm/W.

Figures 4(a), 4(b) and 4(c) show the measured and simulated angle distributions of the light emitted in the regular glass substrate for d_c : 55nm (near the first maximum for η_{out}^{air}), 140nm and 230nm (near the second maximum for η_{out}^{air}), with $d_a = 60$ nm. For the measurements an index-matched half-sphere lens is attached on the substrate and the entire spectrum is measured. The simulation results are for an emission of 530 nm. Note the good agreement between theory and experiment.

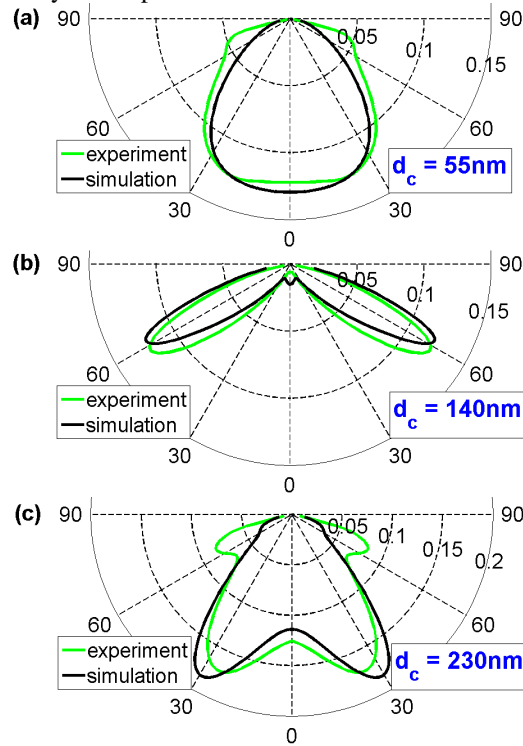


Fig. 4. Measured and simulated angle dependency of the luminance (in the substrate) for three different d_c values: 55nm (a), 140nm (b) and 230nm (c).

4.2 OLED on high refractive index substrate

Now, we will investigate how the use of a high index substrate ($n_{substrate} = 1.8$) affects the light emission of the OLED. As in Figs. 2(a) and 2(b) (for $n_{substrate} = 1.5$) we calculate the outcoupling efficiency in air η_{out}^{air} and in the substrate $\eta_{out}^{substrate}$ as a function of d_c and d_a (Figs. 5(a) and 5(b)). As the refractive index of the substrate is now similar to that of the organic layers, total internal reflection and light trapping in the organic stack are avoided. Figure 5(a) shows that (as for the regular glass substrate) d_c has a stronger influence on η_{out}^{air} than d_a . For the high index substrate, the maximum value for η_{out}^{air} is about 20%, which is slightly lower than the 24% for the regular glass substrate. This is due to a reduction in partial reflection at the ITO/substrate interface, reducing multiple beam interferences. Figure 5(b) shows that the outcoupling efficiency in the substrate $\eta_{out}^{substrate}$ can reach up to 68% if the thickness of the ETL is sufficiently large (d_c larger than 200nm). This outcoupling efficiency is significantly higher than the 42% obtained for a standard glass substrate (compare Figs. 5(b) and 2(b)), because total internal reflection between the organic layers and the substrate does not occur anymore.

Also, the oscillations in $\eta_{out}^{substrate}$ as a function of d_c have completely disappeared (Fig. (6)). The simulations show that most of the absorption takes place in the organic/ITO layers, a smaller amount is absorbed in the silver cathode. If the aim is to enhance the emission into air, it is essential to add an outcoupling structure at the substrate/air interface, to avoid repeated total internal reflection.

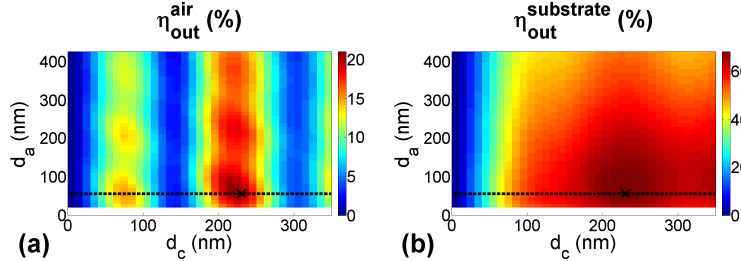


Fig. 5. Simulated outcoupling efficiency in air η_{out}^{air} (a) and in the substrate $\eta_{out}^{substrate}$ (b) for OLEDs with a high index substrate as a function of d_c and d_a i.e. the distances between the emitters and the cathode and the anode respectively. The dashed line ($d_a = 60\text{nm}$) indicates the parameter for which η_{out}^{air} and $\eta_{out}^{substrate}$ are presented on Fig. 8. The cross represents the fabricated OLED with high index substrate with $d_c = 230\text{nm}$ and $d_a = 60\text{nm}$ and for which the maximum luminous efficacy and quantum efficiency was measured (shown on Fig. 6).

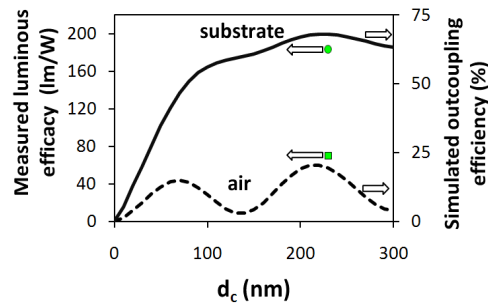


Fig. 6. Measured luminous efficacy (points) in air and in substrate for the best OLED sample on high index substrate with $d_c = 230\text{nm}$ and $d_a = 60\text{nm}$ and simulated outcoupling efficiency (lines) in air η_{out}^{air} and in substrate $\eta_{out}^{substrate}$ as a function of d_c .

Based on the simulation results from Fig. 5, a green emitting $\text{Ir}(\text{ppy})_3$ OLED with $d_c = 230\text{nm}$, $d_a = 60\text{nm}$ (maximizing $\eta_{out}^{substrate}$) and emission area $2.5 \times 2.5 \text{mm}^2$ has been deposited on a high refractive index substrate ($n = 1.8$). The small device area avoids lateral voltage losses in the ITO but the efficiency roll-off for the phosphorescent OLED is still present at higher luminance. Using an integrating sphere and driving the device at 1000cd/m^2 we measured a luminous efficacy of 70lm/W and external quantum efficiency in air of 15%. At the same luminance we found (by attaching an index matched large half-sphere lens on the substrate) a record [13] luminous efficacy of 183lm/W and an external quantum efficiency in the substrate of 42%. This external quantum efficiency is the product of a high outcoupling efficiency (estimated as $\eta_{out}^{substrate} = 68\%$) and a high internal quantum efficiency (estimated as 62%) which is acceptable for $\text{Ir}(\text{ppy})_3$ based emitters [26].

4.3 Comparison of light distribution in layers

The light generated in the emitting layer can have different destinations: emitted in air; trapped in the substrate; absorbed in the organic/ITO layers; or absorbed in the silver electrode. The respective contributions are estimated in Fig. 7 for two devices with same

OLED stack i.e. $d_c = 230\text{nm}$ and $d_a = 60\text{nm}$, one on a regular glass substrate and one on a high index substrate. The fraction of light emitted in air is η_{out}^{air} and the fraction trapped in the substrate is $\eta_{out}^{substrate} - \eta_{out}^{air}$. The fractions absorbed in the silver electrode and absorbed in the organic/ITO layers are obtained from optical simulations. Figure 7 illustrates that the light absorbed in the organic/ITO layers for a high index substrate (29%) is much lower than for regular glass substrate (54%). This is in agreement with the outcoupling of 68% into the high index substrate.

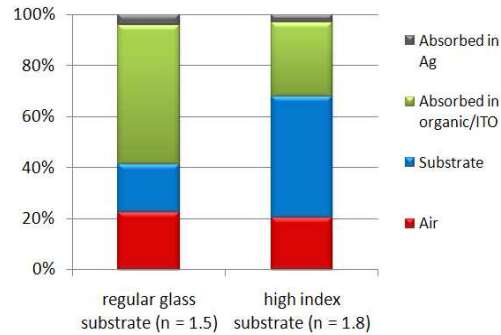


Fig. 7. Simulated fractions emitted into air, trapped in the substrate, absorbed in the organic/ITO layers and absorbed in the silver electrode for an OLED structure ($d_c = 230\text{nm}$ and $d_a = 60\text{nm}$) on regular glass and high index substrate.

4.4 Comparison of electrical properties

Figure 8 compares the current-voltage characteristics of OLED samples on a regular glass substrate and on a high index substrate, both with $d_c = 230\text{nm}$ and $d_a = 60\text{nm}$. The data shows that both devices have the same turn-on voltage, indicating that there is no difference in carrier injection. Because the current-voltage characteristics are nearly identical, we can conclude that there is practically no difference in charge balance. This confirms that the enhanced efficiency of the OLED on a high index substrate is only due to the improved outcoupling efficiency. The ITO on the high index substrate is not deposited in a commercial process and has a larger roughness, leading to a higher leakage current (not shown on Fig. 8) [27] and a higher current below the turn-on voltage.

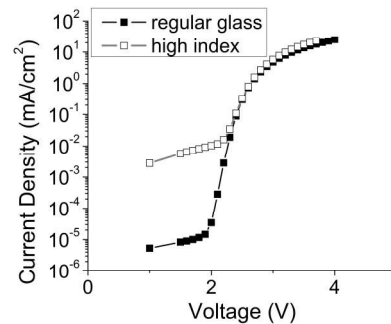


Fig. 8. Measured current- voltage characteristics of OLEDs on a regular glass substrate and on a high index substrate ($d_c = 230\text{nm}$ and $d_a = 60\text{nm}$).

5. Conclusions

In conclusion we have demonstrated that the use of a high refractive index substrate is a promising path for enhancing the outcoupling efficiency (and quantum efficiency and luminous efficacy) of OLEDs. High index substrates eliminate total internal reflection at the

ITO/substrate interface and enable most of the generated light to reach the substrate. Increasing the ETL layer thickness (i.e., distance between the emitters and the cathode) reduces absorption in the metal and further increases the efficiency. Such a thick ETL without a voltage drop can be realized by using electrically doped materials. The simulation results are in good agreement with the efficiency and angle dependency measurements. Using a high index substrate, we could demonstrate an OLED with a record external quantum efficiency of 42% and a luminous efficacy of 183 lm/W into the substrate. These values were measured in an integrating sphere at luminance of 1000cd/m². We plan to investigate the outcoupling of the light from the high index substrate by using a microlens array with a high refractive index on the substrate surface. Another challenge is to optimize a white OLED stack on a high index substrate for lighting applications.

Acknowledgements

The authors would like to thank the European Commission contract IST-004607 (OLLA project) for funding. S.M. and K.N. also acknowledge financial support from the Belgian Interuniversity Attraction Pole on Photonics IAP-VI/10. In addition to EU, Novaled wishes to thank BMBF (Germany) and Saxony for financial support.